White matter alterations in Alzheimer's disease without concomitant pathologies

I. Ferrer*†‡§¶ 🆔 and P. Andrés-Benito*‡¶ 🆔

Department of Pathology and Experimental Therapeutics, University of Barcelona, †Bellvitge University Hospital, ‡Ministry of Economy and Competitiveness, CIBERNED (Network Centre of Biomedical Research of Neurodegenerative Diseases), Institute of Health Carlos III, §Institute of Neurosciences, University of Barcelona and ¶Bellvitge Biomedical Research Institute (IDIBELL), Barcelona, Spain

I. Ferrer and P. Andrés-Benito (2020) *Neuropathology and Applied Neurobiology* **46**, 654–672
White matter alterations in Alzheimer's disease without concomitant pathologies

Aims: Most individuals with AD neuropathological changes have co-morbidities which have an impact on the integrity of the WM. This study analyses oligodendrocyte and myelin markers in the frontal WM in a series of AD cases without clinical or pathological co-morbidities. **Methods**: From a consecutive autopsy series, 206 cases had neuropathological changes of AD; among them, only 33 were AD without co-morbidities. WM alterations were first evaluated in coronal sections of the frontal lobe in every case. Then, RT-qPCR and immunohistochemistry were carried out in the frontal WM of AD cases without co-morbidities to analyse the expression of selected oligodendrocyte and myelin markers. **Results**: WM demyelination was more marked in AD with co-morbidities when compared with AD cases without co-morbidities. Regarding the later, mRNA expression levels of *MBP*, *PLP1*, *CNP*, *MAG*, *MAL*, *MOG* and *MOBP* were preserved at stages I–II/0–A when compared with middle-aged (MA) individuals, but significantly decreased at stages III–IV/0–C. This was accompanied by reduced expression of *NG2* and *PDGFRA* mRNA, reduced numbers of NG2-, Olig2- and HDAC2-immunoreactive cells and reduced glucose transporter immunoreactivity. Partial recovery of some of these markers occurred at stages V–VI/B–C. **Conclusions**: The present observations demonstrate that co-morbidities have an impact on WM integrity in the elderly and in AD, and that early alterations in oligodendrocytes and transcription of genes linked to myelin proteins in WM occur in AD cases without co-morbidities. These are followed by partial recovery attempts at advanced stages. These observations suggest that oligodendrocytopathy is part of AD.

Keywords: Alzheimer disease, co-morbidities, myelin, oligodendrocytes, white matter

Introduction

Reduced white matter (WM) volume, WM lesions and altered WM integrity and cortical disconnection occur in the ageing human brain [1-10]. Age-related WM decay is associated with memory impairment and symptoms of depression in an anatomically specific manner [1-14]. Reduced myelin basic protein (MBP) and 2',3'-cyclic nucleotide 3' phosphodiesterase (CNP) levels [15], and alterations in the number of oligodendrocytes and oligodendroglial precursor cells (OPCs/ NG2-positive cells), have been reported in aged primates and rodents [16].

Reduced WM size, WM hyper-lucencies and myelin and axon damage are common in sporadic Alzheimer's disease (AD), as revealed by neuroimaging methods, mainly magnetic resonance imaging (MRI), and

*Correspondence: Isidro Ferrer, Department of Pathology and Experimental Therapeutics, University of Barcelona, Feixa Llarga sn, 08907 Barcelona, Spain. Tel: 34 94 4035808; Fax: 34 93 4035808; E-mail: 8082ifa@gmail.com

particularly diffusion tensor imaging (DTI) and functional MRI (fMRI) [3-4,12,14,17-22]. Patients with moderate cognitive impairment (MCI) of AD-type exhibit alteration of the WM integrity which further deteriorates with disease progression [5,23-27]. WM alterations appear before the appearance of clinical symptoms [28]. Atrophy of WM, decreased myelin density and demyelination and predominant WM vulnerability of the frontal and parietal lobes are also observed in *post mortem* neuropathological studies [2,29-32]. Myelin loss mainly involves areas that are myelinated late in the development [8,33,34]. Breakdown of WM integrity is considered a principal component of AD, contributing to neural disconnection and progression of clinical symptoms and dementia [13].

However, most studies of WM in the human ageing brain have not considered that in the elderly, most individuals have AD pathology that cannot be visualized with current neuroimaging methods. Therefore, we cannot be certain that a reasonable percentage of aged individuals subjected to neuroimaging studies suffer concomitant AD pathology. Moreover, the presence of a certain number of β-amyloid plaques and neurofibrillary tangles (NFTs) in the elderly have been considered until recently to be normal brain ageing; these cases might have been classified at *post mortem* as normal aged individuals.

Furthermore, co-morbidities are common in the ageing brain and in AD. Vascular cognitive impairment and dementia are prevalent in old age [35-42]. The combination of AD and cerebrovascular disease is very common [43-49]. Other clinical co-morbidities include arterial hypertension (HTA), type II diabetes, cardiac, hepatic and renal failure and respiratory insufficiency; pathological co-morbidities include neurodegenerative disorders with abnormal protein aggregates such as other tauopathies, Lewy body diseases and TDP-43 proteinopathies, among others and hippocampal sclerosis [50-56].

This study was designed to analyse molecular alterations in the WM linked to oligodendrocytes and myelin in cases with AD pathological changes without clinical or pathological co-morbidities. These cases were first selected from a consecutive series of autopsies in a general hospital in which AD was one of the *post mortem* neuropathological diagnoses. Cases with clinical and pathological co-morbidities were not included in the second part of the study.

In the second part of the study, gene transcription was assessed with targeted RT-qPCR, and protein expression of altered genes by immunohistochemistry in the WM of the centrum semi-ovale of the frontal lobe in cases with AD pathology without clinical and pathological co-morbidities at different Braak stages of disease progression. Selected genes for analysis included markers of the oligodendrocyte lineage, genes encoding structural proteins of myelin and genes involved in energy metabolism and axon maintenance. Adult NG2-glia have the capacity to produce myelinating oligodendrocytes [57,58] thus contributing to oligodendrocyte and myelin turnover and regeneration in the adult CNS [59]. Stages of oligodendrocyte lineage are identified by the expression of platelet-derived growth factor receptor α polypeptide (PDGF-Rα), SRY-Box-10 (Sox10), NK2 homeobox 2 (Nkx2.2), oligodendrocyte transcription factor 1 (Olig1) and oligodendrocyte lineage transcription factor 2 (Olig2), among others [60]. After oligodendrocyte differentiation, myelination is triggered by myelin regulatory factor (MYRF) which is expressed in postmitotic oligodendrocytes [61]. Myelination is linked to increased expression of myelin basic protein (MBP), myelin-associated glycoprotein (MAG), proteolipid protein 1 (PLP1), myelin oligodendrocyte glycoprotein (MOG) and 2′, 3′-cyclic nucleotide 3′ phosphodiesterase (CNP), among others [62-68]. Finally, blood-derived glucose is taken up by oligodendrocytes through glucose transporter 1 (GLUT1) encoded by *SLC2A1*. Glucose is metabolized via glycolysis to produce pyruvate and lactate which are delivered to the axons through specific solute carriers, the monocarboxylate transporters (MCT) located in cell membranes [69,70]. MCT1 is mainly expressed in oligodendrocytes [71,72]. Thus, both GLUT1 and MCT1 produced in oligodendrocytes are involved in axon maintenance independently of the complementary myelin/axon trophic alliance. These markers were analysed in this study.

Finally, histone deacetylases (HDACs) remove specific acetyl groups on a histone enabling it to interact with DNA thereby modulating gene transcription. HDAC1 and HDAC2 are expressed in oligodendrocytes [73,74]. HDAC1 immunoreactivity was also assessed in the nuclei of glial cells in the WM.

Our aim was to discern which alterations in the WM in the general population affected by AD pathological changes were linked to AD and not to concomitant clinical and pathological co-morbidities.

Material and methods

Selection of samples

First series Cases for study were obtained at the Bellvitge University Hospital following the guidelines of the Spanish legislation (Real Decreto 1716/2011) and the approval of the local ethics committee. Clinical parameters were retrieved after the revision of the complete clinical history in every case. Only cases with comprehensive clinical information were separated for further analysis. The first series of cases was chosen from consecutive autopsies carried out from 2009 to 2015. The current protocol for the autopsies in adult donors was as follows: one hemisphere was immediately cut in coronal sections, 1 cm thick and selected areas of the encephalon were rapidly dissected, frozen on metal plates over dry-ice, placed in individual air-tight plastic bags and stored at $-80°C$ until use for biochemical studies. The other hemisphere was fixed by immersion in 4% buffered formalin for 3 weeks for morphological studies. For the current neuropathological study, 4-μm-thick sections from 20 representative brain regions were stained with haematoxylin and eosin, periodic acid-Schiff (PAS) and Klüver–Barrera, or processed for immunohistochemistry for microglia Iba1, glial fibrillary acidic protein (GFAP), β-amyloid, phospho-tau (clone AT8), α-synuclein, TDP-43 and ubiquitin, using EnVision + System peroxidase (Dako), and diaminobenzidine and H_2O_2. In addition, 1-cm-thick coronal sections of the frontal lobe at the level of the head of the caudate and putamen were obtained in every case. Blocks were embedded in paraffin, cut at a thickness of 7 μm, de-waxed and stained with haematoxylin and eosin, and with Klüver–Barrera. Details of the 20 selected regions and the methodological protocols for current neuropathological studies are described elsewhere [75]. From among autopsies following this procedure, including the availability of appropriate clinical information and suitability of white matter sections stained with Klüver–Barrera for densitometric studies, 470 of 713 autopsies were initially selected. Three groups were defined. First, all cases with NFT pathology and/or with cerebral β-amyloid deposition, covering NFT pathology stages I–VI of Braak and β-amyloid deposition in the

form of diffuse and/or neuritic plaques Braak stages 0 (no deposits) to C [76], were chosen for further classification. These were 128 men and 78 women (total $n = 206$); mean age ($\pm$SEM): 73.3 $\pm$ 9.6 years. AD cases were categorized as ADI–II/0-A ($n = 113$, men: 83, women: 30; age: 69.1 $\pm$ 8.9 years); ADIII–IV/0–C ($n = 70$, men: 36, women: 34; age: 78.4 $\pm$ 7.6 years) and ADV–VI/B–C ($n = 23$, men: 9, women: 14; age: 78.5 $\pm$ 8.5 years). Most of these cases encompassed a diversity of co-morbidities including metabolic disorders such as HTA, type II diabetes, hyperlipaemia, renal or liver failure and chronic respiratory failure; peripheral and central vascular pathology; age-related neurodegenerative diseases, such as other tauopathies, Lewy body pathology and TDP-43 proteinopathy, among others; hippocampal sclerosis and long agonic state, or vegetative state. Regarding cerebrovascular pathology, cases with cerebral infarcts, including micro-infarcts, lacunes, infarcts in the watershed areas, vascular leucoencephalopathy, hippocampal sclerosis and status cribosus; and cases with severe atherosclerosis, moderate or severe arteriolosclerosis, hypertensive angiopathy, inflammatory vascular diseases and vascular malformations were considered as AD with vascular co-morbidity. This group was classified as AD with concomitant pathology, AD-Co, and was made up of 173 cases, categorized as ADI–II/0–A ($n = 104$), ADIII–IV/0–C ($n = 63$) and ADV–VI/B–C ($n = 7$).

Only 33 of the 206 were classified as cases with AD without co-morbidities. Cases with concomitant mild small blood vessel disease were included in this series. This group was made up of by 15 men and 18 women; age: 76.3 $\pm$ 8.6 years. AD cases without co-morbidities were categorized as follows: ADI–II/0–A ($n = 9$, men: 5, women: 4; age: 68.5 $\pm$ 11.3 years); ADIII–IV/0–C ($n = 8$, men: 2, women: 6; age: 77.7 $\pm$ 4.8 years); ADV–VI/B–C ($n = 16$, men: 8, women: 8; age: 80.7 $\pm$ 5.6 years). All these cases were sporadic; familial AD was not included in this study.

The third group ($n = 20$) was made up of young cases (middle-aged: MA) chosen at random among the remaining 264 cases (470 minus 206). This group consisted of 10 men and 10 women; age: 48.1 $\pm$ 7.7 years. MA did not have the clinical risk factors and co-morbidities mentioned in previous paragraphs; they did not have neurological or mental

diseases, and the neuropathological study did not show abnormalities. The control group must be not interpreted as an age-matched control group, but as a control group of normal WM in MA individuals.

Second series Only cases with AD pathology without co-morbidities were the focus of this part of the study. These cases were the same as those of the second group of the first series. In addition, 10 MA cases (6 men, 4 women; age: 51.7 ± 4.7 years) from the third group of the first series were included and processed in parallel. The total number of MA and AD cases in this series is detailed in Table 1. All these cases were used for specific immunohistochemical studies. However, frozen samples were available for 24 AD cases and 10 controls. In these cases, the brain pH at the time of the autopsy was between 6.2 and 6.4, and the RNA integrity number (RIN) higher than 6 (excepting one case). AD cases at stages I–II/0-A had no neurological symptoms; AD cases at stages III–IV/0–C had no neurological symptoms nor were they affected by mild cognitive impairment; AD cases at stages V–VI/B–C had severe cognitive impairment or dementia.

Quantitative densitometric studies of the WM stained with Klüver–Barrera

Photomicrographs of the centrum semi-ovale of Klüver–Barrera-stained sections, at the level of the head of the caudate and putamen as described above, were obtained at a mid-distance between the inferior frontal sulcus and the cingulate sulcus, approximately at 0.7–1 cm from the external vertex of the lateral ventricle. Figures were obtained at a magnification of × 200, covering an area of 0.126 mm^2, using a DP25 camera adapted to an Olympus BX50 light microscope. The pictures, two areas per case in every case, were analysed using Photoshop software. The density of myelin was calculated as the intensity of blue normalized for the total area and expressed as arbitrary units per area. The normality of distribution was analysed with the Kolmogorov–Smirnov test. Results were analysed with one-way ANOVA and post hoc Tukey. Differences between MA and the two groups of AD, and between the different stages in pure AD cases, were considered statistically significant at *$P < 0.05$, **$P < 0.01$, ***$P < 0.001$ when comparing MA with AD and AD-Co, and $^{\#\#}P < 0.01$ when comparing AD-Co with 'pure' AD.

Table 1. Summary of cases of AD without concomitant co-morbidities and pathologies

Case ID	Diagnosis	Sex	Age	PM delay	RIN WM
1	AD I/0	M	56	07 h 10 min	7.80
2	AD I/A	W	74	02 h 45 min	7.70
3	AD I/A	W	57	05 h 00 min	6.50
4	AD I/A	M	66	09 h 45 min	6.30
5	AD II/0	M	67	07 h 15 min	6.90
6	AD II/0	M	57	04 h 30 min	7.10
7	AD II/A	W	88	08 h 00 min	6.90
8	AD II/A	M	66	04 h 55 min	7.50
9	AD II/A	W	86	02 h 15 min	8.30
10	AD III/0	M	81	01 h 30 min	7.60
11	AD III/0	M	66	05 h 45 min	7.50
12	AD III/0	W	79	03 h 35 min	7.40
13	AD III/A	W	82	02 h 00 min	7.20
14	AD III/A	W	77	03 h 10 min	6.40
15	AD III/B	W	76	03 h 50 min	7.20
16	AD IV/A	W	80	02 h 45 min	5.40
17	AD IV/C	W	81	05 h 00 min	7.30
18	AD V/B	W	74	05 h 30 min	7.70
19	AD V/B	M	86	04 h 15 min	7.90
20	AD V/B	M	73	04 h 30 min	6.90
21	AD V/B	W	82	01 h 45 min	–
22	AD V/B	M	75	11 h 30 min	–
23	AD VI/C	W	72	09 h 30 min	6.40
24	AD VI/C	W	85	16 h 15 min	8.20
25	AD V/C	M	85	03 h 45 min	7.80
26	AD V/C	M	77	16 h 00 min	7.10
27	AD VI/C	W	82	10 h 00 min	–
28	AD V/C	W	86	10 h 00 min	–
29	AD V/C	W	85	12 h 10 min	–
30	AD V/C	M	77	08 h 00 min	–
31	AD V/C	M	79	07 h 30 min	–
32	AD V/C	M	93	03 h 00 min	–
33	AD VI/C	W	81	05 h 15 min	–
34	MA	W	62	11 h 00 min	8.40
35	MA	W	53	03 h 00 min	7.70
36	MA	M	55	05 h 40 min	8.30
37	MA	M	39	09 h 15 min	7.10
38	MA	W	46	14 h 05 min	7.20
39	MA	W	66	04 h 15 min	7.80
40	MA	M	57	03 h 00 min	8.20
41	MA	M	50	17 h 15 min	8.00
42	MA	W	54	06 h 45 min	7.20
43	MA	M	35	17 h 00 min	6.80

RNA purification and RT-qPCR

The WM was dissected from the grey matter in 34 cases, corresponding to 9 ADI–II/0–A, 8 ADIII–IV/0–C, 7 ADV–VI/B–C and 10 MA. WM samples at different AD stages and MA cases were processed in parallel. RNA from frozen WM was extracted following the instructions of the supplier (RNeasy Mini Kit, Qiagen® GmbH, Hilden, Germany). RNA integrity and 28S/18S

ratios were determined with the Agilent Bioanalyzer (Agilent Technologies Inc, Santa Clara, CA, USA). RIN values are shown in Table 1. Samples were treated with DNase digestion, and RNA concentration was evaluated using a NanoDrop™ Spectrophotometer (Thermo Fisher Scientific, Waltham, MA, USA).

TaqMan RT-qPCR assays were performed in duplicate for each gene on cDNA samples in 384-well optical plates using an ABI Prism 7900 Sequence Detection system (Applied Biosystems, Life Technologies, Waltham, MA, USA). For each 10 µl TaqMan reaction, 4.5 µl cDNA was mixed with 0.5 µl 20 × TaqMan Gene Expression Assays and 5 µl of 2 × TaqMan Universal PCR Master Mix (Applied Biosystems). TaqMan probes used in the study are detailed in Table 2. Values of $GUS\text{-}\beta$ were used as internal controls for normalization [77]. The parameters of the reactions were 50°C for 2 min, 95°C for 10 min and 40 cycles of 95°C for 15 s and 60°C for 1 min. Finally, capture of all TaqMan PCR data was made using the Sequence Detection Software (SDS version 2.2.2, Applied Biosystems). For the data analysis, threshold cycle (CT) values for each sample were processed to obtain the double delta CT (ΔΔCT) values. First, delta CT (ΔCT) values were calculated as the normalized CT values for each target gene in relation to the CT of endogenous controls $GUS\text{-}\beta$. Then, ΔΔCT values were obtained from the ΔCT of each sample minus the mean ΔCT of the population of control samples.

The normality of distribution of fold-change values was analysed with the Kolmogorov–Smirnov test. Pearson's correlation coefficient was used to assess a possible linear association between two continuous quantitative variables. To determine the relationship between gene expression and RIN values according to pathologic variables, we used the analysis of covariance (ANCOVA) in the 16 probes. Statistical analysis of the expression data between groups was made using one-way analysis of variance (ANOVA) followed by Tukey posttest, or Kruskal–Wallis test followed by Dunn's post hoc test when required using the SPSS software (IBM Corp. Released 2013. IBM SPSS Statistics for Windows, Version 21.0; Armonk, NY: IBM Corp). Outliers were detected using the GraphPad software QuickCalcs ($P < 0.05$). All data were expressed as mean values ± SEM. Differences between MA and AD cases were considered statistically significant at $*P < 0.05$, $**P < 0.01$, $***P < 0.001$ vs. MA; $^{\#}P < 0.05$,

Table 2. Taqman probes, gene names and identification

Gene	Full name	Reference
CNP	2',3'-cyclic nucleotide 3' phosphodiesterase	Hs00263981_m1
GUS-β	β-glucuronidase	Hs00939627_m1
MAG	Myelin-associated glycoprotein	Hs01114387_m1
MAL	Mal, T-cell differentiation protein	Hs00360838_m1
MBP	Myelin basic protein	Hs00921945_m1
MCT1	Solute carrier family 16 (monocarboxylic acid transporters), member 1	Hs01560299_m1
MOBP	Myelin-associated oligodendrocyte basic protein	Hs01094434_m1
MOG	Myelin oligodendrocyte glycoprotein	Hs01555268_m1
MYRF	Myelin regulatory factor	Hs00973739_m1
NG2	Neural/glial antigen 2	Hs00426981_m1
NKX2-2	NK2 Homeobox 2	Hs00159616_m1
OLIG1	Oligodendrocyte transcription factor 1	Hs00744293_s1
OLIG2	Oligodendrocyte lineage transcription factor 2	Hs00377820_m1
PDGFRA	Platelet-derived growth factor receptor, alpha polypeptide	Hs00998018_m1
PLP1	Proteolipid protein 1	Hs00166914_m1
SLC2A1	Solute carrier family 2 (facilitated glucose transporter), member 1	Hs01102423_m1
SOX-10	SRY-box 10	Hs00366918_m1

$^{\#\#}P < 0.01$, $^{\#\#\#}P < 0.001$ vs. ADI–II/0-A and $^{\$}P < 0.05$ vs. ADIII–IV/0–C and ADV–VI/B–C.

Immunohistochemistry

Formalin-fixed, paraffin-embedded, de-waxed sections 4-µm thick of the frontal white matter of cases listed in Table 1 were processed for specific immunohistochemistry. The sections were boiled in citrate buffer (20 min) to retrieve protein antigenicity. Endogenous peroxidases were blocked by incubation in 10% methanol, 1% H_2O_2 solution (15 min) followed by 3% normal horse serum solution. Then the sections were incubated at 4°C overnight with one of the primary rabbit polyclonal antibodies: NG2 (used at a dilution of 1:200; Sigma-Aldrich, Merck, Darmstadt, GE), Olig2 (used at a dilution of 1:500, Sigma-Aldrich, Merck); HDAC2 (diluted 1:100, Abcam, Cambridge, UK); GLUT 1 (diluted 1:100, Abcam); or with one of the primary mouse monoclonal antibodies: PLP1 (used at a dilution of 1:100, Lifespan Biosci, Seattle, WA, USA), CNPase (used at a dilution of 1:100, Sigma-Aldrich, Merck), MBP (diluted 1:1000, Abcam) and GFAP (diluted

1:1000, Diagnostic BioSyst, CA, USA). Following incubation with the primary antibody, the sections were incubated with EnVision + system peroxidase (Dako, Agilent Technologies, Santa Clara, CA, USA) for 30 min at room temperature. The peroxidase reaction was visualized with diaminobenzidine and H_2O_2. Control of the immunostaining included omission of the primary antibody; no signal was obtained following incubation with only the secondary antibody. Sections were slightly counterstained with haematoxylin.

Quantification of NG2-, Olig2- and HDAC2-immunoreactive cells in the WM was done by counting the number of positive cells in areas of the WM located about 1 cm below the subcortical U fibres of the frontal lobe at the level of the head of the caudate and putamen chosen at random. Microphotographs were obtained at magnifications of × 200 or × 400, covering areas of 0.126 mm^2 and 0.038 mm^2, respectively, in three nonconsecutive sections per case using a DP25 camera adapted to an Olympus BX50 light microscope. The number of positive cells was counted directly on the figures and expressed as the number of positive cells per area (0.038 mm^2 for NG2- and HDAC2-immunoreactive cells, and 0.126 mm^2 for Olig2-positive cells). The normality of distribution of fold-change values was analysed with the Kolmogorov–Smirnov test. Results were analysed with one-way ANOVA and post hoc Tukey; differences were considered statistically significant at * MA *vs.* AD; #: ADI–II *vs.* ADIII–IV or ADV–VI; $: ADIII–IV *vs.* ADV–VI; significance levels were set at: *, # $P < 0.05$, **, ## $P < 0.01$, and ***, ###, $$$ $P < 0.001$. No attempts were made to quantify the densitometry of GLUT1.

Densitometric quantification of PLP1 immunoreactivity was acquired in the same areas as those indicated for NG2-, Olig2- and HDAC2-immunoreactive cells following a similar procedure to that described for Klüver–Barrera-stained sections. Photomicrographs were obtained at a magnification of × 200, covering an area of 0.126 mm^2, using a DP25 camera adapted to an Olympus BX50 light microscope. The pictures, two areas per case in every case, were analysed using Photoshop software. The density of PLP1 was calculated as the intensity of brown colour normalized by the total area excluding white spaces of the nuclei and expressed as arbitrary units per area. The normality of distribution was analysed with the Kolmogorov–Smirnov test. Results were analysed with one-way ANOVA

and post hoc Tukey. Differences between MA and the three stages of pure AD cases were considered statistically significant at: * MA *vs.* AD; #: ADI–II *vs.* ADIII–IV or ADV–VI; $: ADIII–IV *vs.* ADV–VI. Significance levels were set at: *, # $P < 0.05$, **, ## $P < 0.01$ and ***, ###, $$$ $P < 0.001$.

Results

White matter alterations in the general series

Representative examples of the diversity of WM changes in cases with AD pathology without and with co-morbidities (AD-Co) are shown in Figure 1. This illustrates the variability in WM alterations which may concur in cases with AD pathology.

Densitometric studies of the central myelin were carried out in the AD series and in MA (Figure 2A). The density of myelin was significantly reduced in AD without co-morbidities and in AD-Co when compared with MA ($P = 0.000$ and $P = 0.000$ respectively). Myelin density was significantly lower in AD-Co when compared with AD cases without co-morbidities ($P = 0.003$) (Figure 2B).

Regarding AD cases without co-morbidities, no significant differences, but rather a tendency to reduced myelin density was seen in AD stages V–VI when compared with AD stages I–II and AD stages III–IV (Figure 2C).

RNA expression of genes related to oligodendroglia and myelin in WM of AD without co-morbidities

Results of RT-qPCR are summarized in Figure 3. The expression of several genes linked to the oligodendrocyte lineage was reduced at stages III–IV/0–C when compared with MA and with AD stages I–II/0-A including *OLIG1* ($P = 0.007$, when compared with ADI–II/A–C) and *PDGFRA* ($P = 0.000$ when compared with MA, and $P = 0.029$ when compared with ADI–II/0-A). Levels of *PDGFRA* were decreased at stages V–VI/B–C when compared with MA ($P = 0.000$); *PDGFRA* and *OLIG1* levels were also significantly decreased at stages V–VI/B–C when compared with levels at stages ADI–II/0-A ($P = 0.015$ and $P = 0.002$ respectively). Curiously, *NG2* mRNA expression was reduced only at stages ADV–VI/B–C when compared with levels of MA and AD stages I–II/0-C ($P = 0.006$ and $P = 0.027$ respectively).
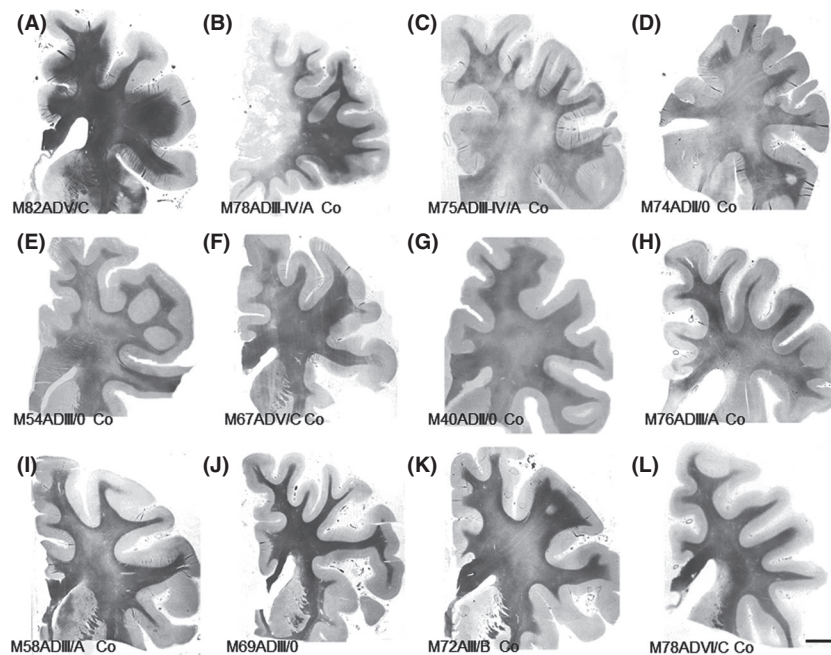
Figure 1. Representative formalin-fixed, paraffin-embedded, de-waxed coronal sections of the frontal cortex at the level of the head of the caudate and putamen, stained with Klüver–Barrera. (**A**) AD stage V/C, the absence of co-morbidities (M, 82y); (**B**) ADIII–IV/A presenting with a frontal infarct (M, 78y); (**C**) Patient categorized as mixed dementia suffering from HTA and extensive WM hyper-lucencies, AD stage III–IV/A, LBD stage 3 (M, 75y); (**D**) Patient with chronic respiratory insufficiency and terminal hypoxia, AD pathology stage II/0 (M, 74y); (**E**) Patient with chronic respiratory failure, abnormal behaviour of nondetermined origin and AD- pathology stage III/0 (M, 54y); (**F**) Patient with cognitive impairment, focal WM hyper-lucencies, lacunar infarcts, HTA and AD stage V/C (M, 67y); (**G**) Patient with cognitive impairment, HTA, WM hyper-lucencies and AD pathology stage II/0 (M, 40y); (**H**) Patient with severe cognitive impairment, type II diabetes, hyperlipidaemia, obesity, HTA, renal failure, argyrophilic grain disease stage II and AD pathology III/A (M, 76y); (**I**) Patient with hepatic encephalopathy and AD pathology stage III/A (M, 58y); (**J**) Patient with no neurological symptoms, and the absence of clinical and pathological co-morbidities, categorized as AD stage III/A (M, 69y); (**K**) Patient with mild cognitive impairment, WM hyper-lucencies, HTA and AD pathology stage III/B (M, 72y); (**L**) Patient with long-lasting dementia, the absence of risk factors of cerebral circulatory disturbance, and affected by ADVI/C, argyrophilic grain disease stage II and TDP-43 proteinopathy (M, 76). The figure makes it evident that there is variable involvement of the WM in association with distinct cerebral and systemic disorders concomitant with AD pathology. M: man. Compare the variability of WM involvement in cases **B**, **C**, **E**, **H**, **I** and **K** categorized as AD with co-morbidities (AD-Co) with **J** categorized as AD without co-morbidities, all of them stage ADIII–IV of Braak and Braak. Cases **D** and **G**, classified as AD-Co stage II, also show decreased staining of the centrum semi-ovale when compared with stage III of AD without co-morbidities (**J**). Differences are also observed between AD without co-morbidities stage V (**A**) in comparison with AD-Co stages V and VI (**F** and **L**). Note that all cases in the figure correspond to males to avoid gender bias).

However, other markers of oligodendrocyte differentiation such as *SOX10* and *NKX-2*, as well as *OLIG2*, were not significantly altered, although *OLIG2* showed a trend to decrease at middle stages of AD.

Regarding genes involved in myelin synthesis, *MYRF* mRNA expression, the product of which triggers myelination, was significantly increased in ADI–II/0-A and ADV–VI/B–C when compared with MA ($P = 0.002$ and $P = 0.033$ respectively). *MYRF* expression was transiently reduced to normal levels at stages III–IV/0–C when compared with ADI–II/0-A and ADV–VI/B–C ($P = 0.005$ and $P = 0.049$ respectively). In contrast, the majority of genes which encode proteins of the myelin sheet showed reduced expression levels at AD stages III–IV/0-C when compared with MA or with AD stages I–II/0-C: *MBP* ($P = 0.009$ when compared with MA), *PLP1* ($P = 0.003$ when compared with AD stages I–II/0-A), and *CNP*, *MAG*, *MAL*, *MOG* and *MOBP* when compared with MA ($P = 0.006$, $P = 0.005$, $P = 0.006$, $P = 0.035$ and $P = 0.041$ respectively). Curiously, the mRNA expression levels of several myelin-related genes were within normal values at AD stages V–VI/B–C, including *MBP*, *PLP1*, *CNP*, *MAL*, *MOG* and *MOBP*. Yet levels of *MAG* were decreased in ADV–VI/B–C when compared with MA ($P = 0.032$) (Figure 3).

The expression of the gene coding for glucose transporter (*SLC2A1*) was reduced in ADV–VI/B–C when compared with MA ($P = 0.039$). In contrast, the
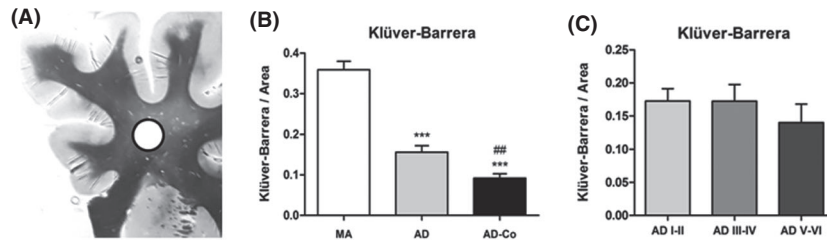
Figure 2. Densitometric values of myelin sheet phospholipids as revealed in Klüver–Barrera-stained sections of the centrum semi-ovale at the level of the head of the caudate and putamen in MA, AD with co-morbidities (AD-Co), and cases of AD without co-morbidities (AD). Values are expressed as arbitrary units per area. (**A**) The area of densitometric studies is indicated by the circle; Klüver–Barrera staining in an MA case. Note that the area is separated from the periventricular white matter and the subcortical U-fibres. (**B**) Significant decrease in AD without co-morbidities ($n = 33$) and AD-Co ($n = 173$) is seen when compared with MA ($n = 20$). The intensity of myelin staining is significantly lower in AD-Co when compared with AD cases. (**C**) No significant differences, but a tendency to reduced myelin intensity is seen in AD without co-morbidities at stages V–VI/B–C (ADV–VI) when compared with AD at stages I–II/0-A (ADI–II) and AD at stages III–IV/0-C (ADIII–IV). ADI–II/0-A, $n = 9$; ADIII–IV/0-C, $n = 8$; ADV–VI/B–C, $n = 16$. One-way ANOVA and post hoc Tukey, ***$P < 0.001$ AD and AD-Co compared with MA; ##$P < 0.001$: AD-Co compared with AD without co-morbidities.
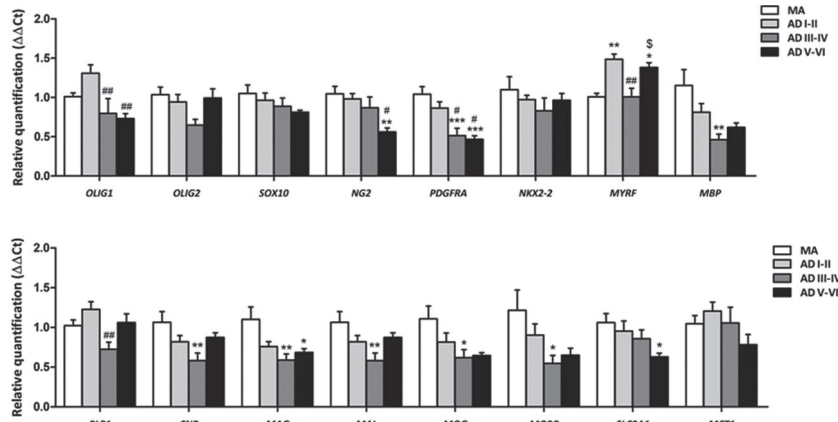

Figure 3. mRNA expression of selected oligodendrocyte- and myelin-related genes in the frontal white matter of MA, AD without co-morbidities stages I–II/0-A (ADI–II), III–IV/0-C (III–VI) and V–VI (B, C). Abbreviations may be seen in Table 2. One-way analysis of variance (ANOVA) followed by Tukey posttest or Kruskal–Wallis test followed by Dunn's post hoc test when required using the SPSS software; *$P < 0.05$, **$P < 0.01$, ***$P < 0.001$ *vs.* MA; #$P < 0.05$, ##$P < 0.01$ *vs.* ADI–II; $$P < 0.05$ *vs.* ADIII–IV and ADV–VI (see Methods for statistical studies).

expression levels of *MCT1*, the gene coding for solute carrier family 16 (monocarboxylic acid transporter, member 1), were not significantly altered, but did show a trend to reduction at advanced stages of AD (Figure 3).

Immunohistochemistry

NG2 (which identifies oligodendroglial precursor cells) immunoreactivity in the WM was detected as small granules in the cytoplasm of a subpopulation of glial cells, whereas Olig2 (which is expressed in oligodendrocytes) immunoreactivity decorated the nucleus of oligodendrocytes. The number of NG2-positive cells

decreased with disease progression, but significant differences were detected only between ADI–II/0-A when compared with ADIII–IV/0-C ($P = 0.001$), and between ADI–II/0-A compared with ADV–VI/B–C ($P = 0.000$). Olig2-positive cells also decreased with disease progression: MA *vs.* ADIII–IV/0–C ($P = 0.011$), MA *vs.* ADV–VI/B–C ($P = 0.000$), ADI–II/0-A *vs.* ADIII–IV/0–C ($P = 0.016$), ADI–II/0-A *vs.* ADV–VI/B–C ($P = 0.000$) and ADIII–IV/0–C *vs.* ADV–VI/B–C ($P = 0.000$). Moreover, Olig2-immunoreactive cells with large, dense and often elongated nuclei were found in ADV–VI/B–C (Figure 4, Figure 6).

HDAC2 immunoreactivity was found in the nucleus of glial cells. The number of HDAC2-positive cells and

the intensity of the staining in the remaining cells significantly decreased with disease progression: MA *vs.* ADIII–IV/0–C ($P = 0.007$), MA *vs.* ADV–VI/B–C ($P = 0.000$), ADI–II/0-A *vs.* ADIII–IV/0-C ($P = 0.035$); ADI–II/0-A *vs.* ADV–VI/B–C ($P = 0.000$), and ADIII–IV/0-C *vs.* ADV–VI/B–C ($P = 0.000$) (Figures 4 and 6).

GLUT1 (glucose transporter member 1) immunoreactivity, which decorated the neuropil and the wall of the small blood vessels, decreased in AD with disease progression. However, no attempt was made to quantify the density of the immunostaining due to individual variations (Figure 4).

Regarding myelin proteins, the intensity of PLP1, CNPase and MBP immunoreactivity decreased with disease progression (Figure 5). Densitometric studies were carried out only for PLP1. Significant reduction was observed in ADI–II/0-A, ADIII–IV/0–C and ADV–VI/B–C when compared with MA ($P = 0.000$, $P = 0.000$ and $P = 0.002$ respectively). Moreover, significant differences were also seen between ADI–II/0- *vs.* ADIII–IV/0-C ($P = 0.000$) and ADIII–IV/0-C *vs.* ADV–VI/B–C ($P = 0.000$) (Figure 6).

In contrast, GFAP immunoreactivity showed an increase in the number and intensity in individual astrocytes in the WM in parallel sections (data not shown), in agreement with previous data from several authors, as reviewed elsewhere [78].

Discussion

This study was designed to learn about WM abnormalities in cases with AD pathology without co-morbidities
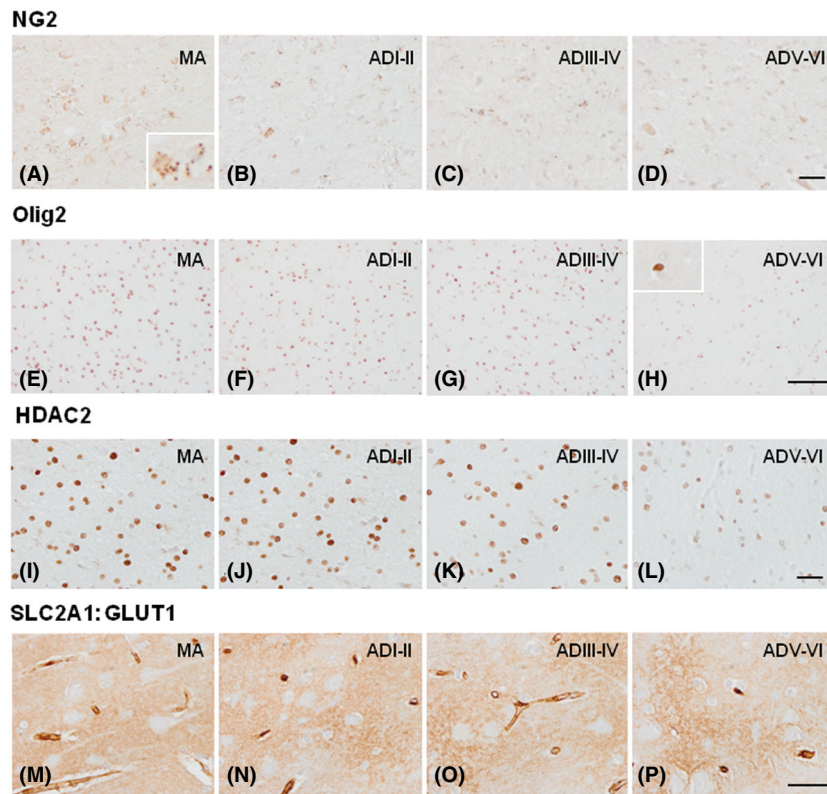

Figure 4. Immunohistochemistry to cellular markers NG2, Olig2, HDAC2 and SLC2A1:GLUT1 in MA individuals (**A, E, I, M**), and in cases with AD without co-morbidities at stages ADI–II/0-A (ADI–II) (**B, F, J, N**), ADIII–IV/0–C (ADIII–IV) (**C, G, K, O**) and ADV–VI/B–C (ADV–VI) (**D, H, L, P**). Decreased numbers of NG2-, Olig2- and HDAC2-immunoreactive cells are observed at middle, and particularly, advanced stages of AD. Large hyperchromatic Olig2-positive cells are also observed in ADV–VI. GLUT1 immunoreactivity is manifested as a fine uniform meshwork in the neuropil which is progressively disrupted into patches of variable immunoreactivity with disease progression. Paraffin sections, slightly counterstained with haematoxylin; NG2, HDAC2, bar = 50 μm; Olig2 and SLC2A1, bar = 45 μm. Insert in MA NG2 is at greater magnification to show small positive granules characteristic of NG2 immunoreactivity. Insert in Olig2 ADV–VI shows a representative large hyperchromatic Olig2-immunoreactive cell; these cells are commonly present in ADV–VI.
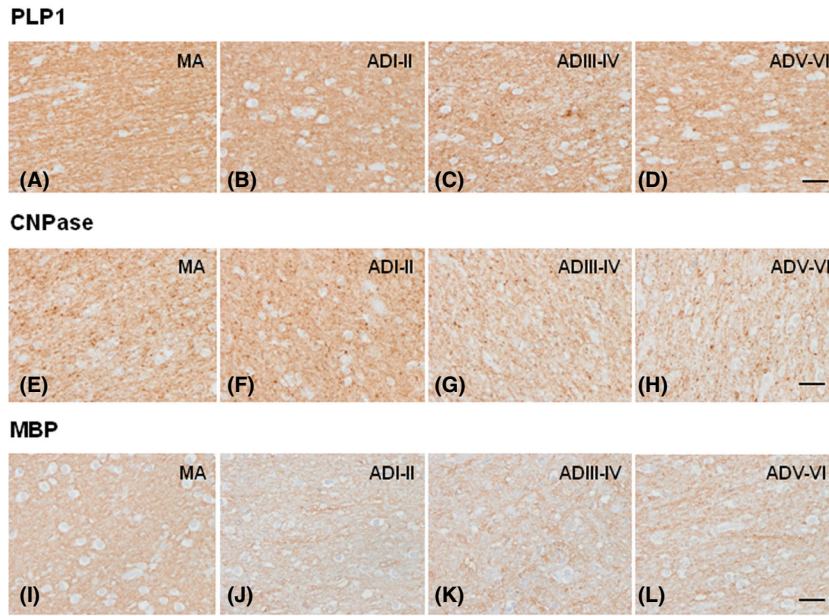
Figure 5. Immunohistochemistry to myelin markers PLP1, CNPase and MBP in the centrum semi-ovale of the frontal lobe in MA (**A**, **E**, **I**), and in cases with AD without co-morbidities at stages ADI–II/0-A (ADI–II) (**B**, **F**, **J**), ADIII–IV/0-C (ADIII–IV) (**C**, **G**, **K**) and ADV–VI/B–C (ADV–VI) (**D**, **H**, **L**). Representative images show reduced immunoreactivity with disease progression, and small PLP1- and CNPase-immunoreactive dots in ADV–VI. Paraffin sections, slightly counterstained with haematoxylin; bar = 50 μm.
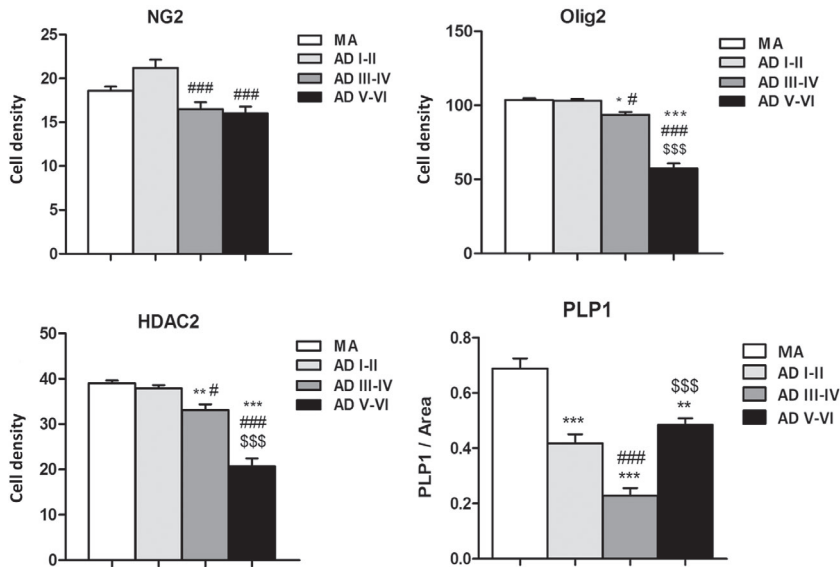

Figure 6. Quantitative study of NG2-, Olig2- and HDAC2-immunoreactive cells in the frontal WM per area of AD cases without co-morbidities (0.038 mm^2 for NG2- and HDAC2-immunoreactive cells, and 0.126 mm^2 for Olig2-positive cells; see Methods). The number of positive cells decreases with increasing stages of AD pathology. MA, $n = 10$; ADI–II/0-A, $n = 9$; ADIII–IV/0-C, $n = 8$; ADV–VI/B–C, $n = 16$. One-way ANOVA and post hoc Tukey; *: MA *vs.* ADIII–IV/0-C (ADIII–IV) or ADV-VI/B–C (ADV–VI); #: ADI–II/0-A (ADI–II) *vs.* ADIII–IV or ADV–VI; $: ADIII–IV *vs.* ADV–VI; significance level set at *, # $P < 0.05$, ** $P < 0.01$ and ***, ###, $$$ $P < 0.001$.

at different stages of disease progression. For this purpose, our first approach was to consider all cases in which one of the *post mortem* neuropathological diagnoses was AD pathology in a continuous series of necropsy cases in a general hospital. Following this procedure, 206 of the 470 cases with adequate clinical

information and histological quality to carry out densitometric studies of the WM of the frontal lobe were selected. Interestingly, 89% of cases aged 65 and older had AD pathology, a slightly higher figure than the percentage already reported for this age group [79,80]. Review of the clinical history and neuropathological study revealed that 84% had concomitant cerebrovascular pathology; clinical morbidities such as HTA, type II diabetes, hyperlipaemia, renal or liver failure and chronic respiratory failure; cerebrovascular pathology; age-related neurodegenerative diseases, such as other tauopathies, Lewy body pathology and TDP-43 proteinopathy; and long agonic state, or vegetative state, which were putative causes of WM alterations. After further selection, 33 were categorized as AD cases without co-morbidities.

It can be argued that not all AD cases had cognitive impairment and dementia, and therefore, they cannot be classified as AD. Moreover, six cases of AD stages I–III without co-morbidities did not have β-amyloid deposits, and they might be classified as Primary age-related tauopathy (PART) [81]. However, PART has also been considered as part of AD [82]. We have followed here this consideration because AD and PART share the same NFT pathology at early stages of the disease.

Densitometric analysis performed on Klüver–Barrera-processed sections of the central WM of the frontal lobe at the level of the head of caudate and putamen revealed significant differences between MA individuals and cases with AD. It is important to stress that the MA group was composed of individuals with an age of about 25 years younger than that of the AD groups. Therefore, MA must be not considered an age-matched control group, but rather a representation of the myelin in normal MA individuals. A significant reduction in phospholipid myelin in elderly, as revealed with Klüver–Barrera staining, is consistent with the idea that myelin in the cerebral WM decreases with age, as already noted in the Introduction. Since the majority of individuals aged 65 and older had AD pathology, it is difficult to ascertain whether changes in the AD groups were linked to ageing or associated with AD pathology.

More practical is the observation that myelin decay is greater in AD cases with co-morbidities (AD-Co) than in AD cases with no co-morbidities. The age of the individuals has been assessed in every case, and the mean values ± SEM have been obtained for every stage both in the total series and in pure AD. Values are similar in both groups, and then comparisons are not biased by differences in the age, but in the presence or absence of co-morbidities. Since the majority of cases with AD in our series had co-morbidities, it may be inferred that part of the WM lesions commonly reported in the elderly and in AD during life cannot be ascribed solely to age and AD, but rather to common concomitant risk factors and pathologies affecting the ageing brain.

Biochemical alterations in WM in AD without co-morbidities

Previous studies have shown alterations in the lipid composition of the WM in AD. Galactosylceramide (Gal-Cer) and sulphatides, synthesized by oligodendroglia in the CNS, are major components of myelin. Reduced Gal-Cer and sulphatide levels, increased cholesterol and increased fatty acid contents occur in cortical grey and WM in AD [83-88]. Levels of GalCer and sulphatide slightly decreased in the frontal and temporal cortex, and in WM matter at stages III–IV, and more markedly at stages V–VI in AD [89]. Curiously, the activity of ceramide synthase 2, which catalyses the synthesis of very long chain ceramides, decreased in brain temporal cortex at stages I–II and frontal cortex at stages III–IV preceding neurofibrillary tangle formation, suggesting that alterations of ceramide synthesis occur earlier than previously suspected in the spread of AD [89]. Our observations on Klüver–Barrera-stained sections are in line with biochemical studies showing decreased levels of phospholipid components of myelin in AD when compared with MA individuals. Differences are not as clear among stages in AD cases without co-morbidities, although a trend to reduction is observed at advanced stages.

Regarding myelin proteins, progressive reduction in the levels of myelin basic protein (MBP), myelin proteolipid protein (PLP) and 2′,3′-cyclic nucleotide 3′-phosphodiesterase (CNP) has been reported in the WM of the parietal and occipital lobes in AD correlating with Braak stages V–VI [90]. Reduced levels of CNP have also been recorded in the WM of the frontal lobes in advanced AD [89,90].

Our observations are restricted to cases with AD pathology without co-morbidities. mRNA expression levels of *MBP*, *PLP1*, *CNP*, *MAG*, *MAL*, *MOG* and *MOBP* were preserved in the frontal white matter at stages I–II/0-A when compared with MA, but they were transiently decreased at stages III–IV/0-C, and

increased thereafter to reach nearly MA levels at stages V–VI/B–C. Regarding protein expression, densitometric studies of PLP1 in the same region revealed a significant decrease in PLP1 immunoreactivity at early stages of AD, which became more marked at middle stages, followed by a slight increase without reaching MA values at advanced stages of AD.

It is worth to stress that differences between AD stages are not related to the age or gender of the individuals, but rather to the stage of the disease. Differences between myelin lipids, as revealed with Klüver–Barrera staining, and myelin proteins as shown by RT-qPCR and immunohistochemistry, in the same cases may be related to differing preciseness of the methods employed. However, the relative recovery of myelin proteins, but not of phospholipids, at advanced stages of the disease deserves further study, including analysis of a possible structural imbalance between lipid and protein components of the myelin sheet in the elderly and in AD. Studies in the aged human *post mortem* brain have shown decreased internodal distance, reduced axon thickness and greater vulnerability of thin myelinated fibres compared with large myelinated fibres [7]. Little is known about this aspect in AD.

β-amyloid and tau

It has been suggested that cortical atrophy with neuron loss is not the main cause of WM damage in AD, as revealed by pioneering neuropathological studies [29], and later supported by combined MRI and *post mortem* examination [9,91]. However, this hypothesis has been brought into question by other studies. The impact of β-amyloid on oligodendrocytes is equivocal. On the one hand, β-amyloid is toxic to oligodendrocytes as identified in *in vitro* models, transgenic mice and familial AD [92-96]. However, Aβ oligomers also promote oligodendrocyte differentiation and maturation in isolated oligodendrocytes and in organotypic cerebellar slices [97]. In fact, deterioration of the WM parallels, but does not correlate with either the total amount or the regional localization of β-amyloid plaques [98]. However, soluble β-amyloid is abundant in the WM in the absence of plaques in AD [99]. Therefore, the possibility of oligodendrocyte damage by soluble β-amyloid in AD cannot be ignored.

WM damage has been correlated with tau pathology in the cerebral cortex [10,101]. Therefore, myelin breakdown in AD has been posited as being linked to axonopathy and transport deficits [10-102]. In favour of WM axonopathy resulting from tau pathology is the presence of WM breakdown in transgenic mice bearing the P301L mutation in the *mapt* gene [13]. Yet, WM disruption does not correlate exactly with the localization and distribution of NFTs in AD [29]. The present findings further support the concept of early alteration of the WM in AD, as transcription of oligodendrocyte and myelin genes in the frontal WM is altered at stages III–IV/0–C at which point no NFTs or neuron loss are found in this region.

Oligodendrocytes and NG2-glia

Previous studies have shown reduced size of the nuclei of oligodendrocytes [14], and decreased numbers of Olig2- and NG2-glia-immunoreactive cells [15,106]. Moreover, several oligodendroglial nuclei in the WM show oxidative damage (8-OHdG immunoreactivity), whereas other oligodendrocytes exhibit increased expression of p53 as a marker of stress, and a senescent phenotype (SA-β-gal immunoreactive) [17,108].

Reduction in the expression of *NG2* and *PDGFRA* mRNA (stages V–VI/A–C, and stages III–IV/0–C and V–VI/A–C respectively), together with reduced numbers of NG2- and Olig2-immunoreactive cells in the WM, points to progressive decline of the oligodendrocyte lineage in the frontal WM with disease progression, which is in line with the demonstration of early alterations of the oligodendrocyte lineage linked to AD pathology [15,106].

Reduction in NG2-glia is important as it probably compromises the regenerative ability of the WM to restore the number of oligodendrocytes and myelin homeostasis. Reduced numbers of oligodendrocytes and altered control of glucose and lactate metabolites necessary for trophic support for axons may produce, in turn, altered axonal function, and axonal degeneration. This scenario takes place at a limited rate in the ageing human brain [19], but its potentially damaging effect is overwhelmed in AD [110].

Histone deacetylases (HDACs) remove specific acetyl groups on a histone enabling it to interact with DNA thereby modulating gene transcription. Increased HDAC2 facilitates oligodendrocyte differentiation [73,74]. Thus, HDAC2 reduction likely compromises oligodendrogenesis.

An intriguing feature in this scenario is the increased expression of *MYRF* mRNA at early and late stages of AD. Regarding the number of oligodendrocytes, reduced expression of *MYRF* mRNA could be expected, whereas with MYRF being a factor regulating the expression of several myelin genes, the expression of such genes would be expected to increase in AD. We have no explanation for the altered MYRF regulation and response in AD.

Transgenic mice expressing β-amyloid and tau as animal models to uncover WM abnormalities in AD

WM alterations have also been examined in several types of transgenic mice carrying the APP/PS1 (K670N/M671L Swedish and PS1dE9) mutation, PS1 mutation, and 5xFAD mutation (Swedish mutation, 1716V Florida mutation, V717I London mutation, and PS1 with M146L and L286V mutation), as well as 3xTg-AD mice (APP Swedish mutation, a presenilin knock-in mutation and P301L tau) [111-117].

In all these models, WM alterations characterized by myelin loss and decreased numbers of oligodendrocytes occur at early stages before the appearance of β-amyloid plaques, and they increase for a limited period of disease progression. Oligodendroglial cell death and myelin loss occur at early stages in 3xTg-AD mice [112,113], and region-specific alterations appear before β-amyloid and tau pathology [112]. However, murine models of β-amyloid deposition show reparative responses at later stages of the disease [15,114-116]. No similar increase in Olig2 and NG2-immunoreactive cells occurs in AD, as shown in the present work and in previous studies [15-106,109,110]. However, a certain normalization of the mRNA expression of several myelin-related genes here observed in AD without co-morbidities has its counterpart in transgenic models. As a working hypothesis, it may be suggested that repair of oligodendrocyte lineage is activated in AD and transgenic models, but regeneration is minimized in AD when compared with transgenic murine models.

Vascular alterations in ageing and AD

Vascular and circulatory alterations including atherosclerosis, small blood vessel disease, tortuous and coiled arterioles, reduced vascular density and cerebral complications such as micro-infarcts, hypoperfusion and micro-bleeds are common in aged human brains [4,118-123].

In addition to vascular alterations linked to age, which may occur in any patient, hypoperfusion linked to β-amyloid deposition, alteration of the blood vessel walls, increased RAGE, altered microglia and astrocytes with senescent forms are constant in AD. β-amyloid angiopathy is found in the vast majority of cases [124,125] and it shows an early predilection for cortical blood vessels. β-amyloid deposition is accompanied by decreased expression of efflux receptor for β-amyloid and increased influx receptor RAGE in AD [126,127]. Other alterations include atrophy, oedema and increased numbers of pinocytic vesicles in endothelial cells; thickening and focal disruption of the basal membrane; increase in heparan sulphate, proteoglycans, collagen IV and laminin in the basal membrane, with atrophy of smooth muscle fibres and augmented aquaporin expression in perivascular astrocytes [128-132]. These changes, in conjunction with mounting evidence of altered blood–brain barrier in AD [133-136], lend support to the old proposal of reduced perfusion of the brain as a pathogenic factor in AD [137-139].

Our study in AD cases without co-morbidities excludes major vascular pathology and systemic circulatory factors which could have an impact on the integrity of oligodendrocytes and myelin. However, we cannot rule out a role for primary alterations in blood vessels linked to AD since specific vascular pathology is one of the manifestations of AD.

Conclusions

WM alterations in AD have been considered the result of cerebrovascular dysfunction [138,139], axonopathy linked to retrograde neuronal tau deposition [10-102], or homeostatic responses to age-related myelin breakdown [140]. These factors are not mutually exclusive, but rather reinforce each other with age and disease progression. This study has tried to minimize co-morbidities in a general population with AD pathology dying in a general hospital. It may be argued that: i. the population dying in a general hospital is not representative of the total population whose health status is better than that represented by in-patients, and that co-morbidities are less frequent and serious in the general population when compared with individuals dying in the hospital; and ii. vascular ageing, and of course

vascular changes linked to AD, cannot be ruled out in the pathogenesis of WM disorders in the present series of AD cases without co-morbidities. These are undoubtedly reasonable objections.

Yet, several studies have stressed the role of oligodendrocytes as important players in the pathogenesis of distinct neurodegenerative diseases including AD [141-144]. In this line, the present observations point to early alterations of oligodendrocytes and transcription of genes linked to myelin proteins in WM in cases with AD pathology without co-morbidities before the appearance of NFTs in these regions, and before the appearance of clinical symptoms of cognitive impairment. This suggests that oligodendrocytes are along with neurons, targets of AD, and that oligodendrocytopathy is therefore part of AD.

Author contributions

IF designed the study, revised the neuropathology of cases, selected the cases without co-morbidities, interpreted the results and wrote the manuscript; PAB carried out the RT-qPCR studies and immunohistochemistry. Both authors revised and approved the final version of the manuscript.

Disclosure

The authors declare that they do not have conflict of interest.

Funding information

Data availability statement

Data sharing is not applicable to this article as no new data were created or analysed in this study.

References

1 Hachinski VC, Potter P, Merskey H. Leuko-araiosis. *Arch Neurol* 1987; **44**: 21–3

2 Scheltens P, Barkhof F, Leys D, Wolters EC, Ravid R, Kamphorst W. Histopathologic correlates of white matter changes on MRI in Alzheimer's disease and normal aging. *Neurology* 1995; **45**: 883–8

3 Barber R, Scheltens P, Gholkar A, Ballard C, McKeith I, Ince P, et al. White matter lesions on magnetic resonance imaging in dementia with Lewy bodies, Alzheimer's disease, vascular dementia, and normal aging. *J Neurol Neurosurg Psychiat* 1999; **67**: 66–72

4 Holland CM, Smith EE, Csapo I, Gurol ME, Brylka DA, Killiany RJ, et al. Spatial distribution of white-matter hyperintensities in Alzheimer disease, cerebral amyloid angiopathy, and healthy aging. *Stroke* 2008; **39**: 1127–33

5 Salat DH, Greve DN, Pacheco JL, Quinn BT, Helmer KG, Buckner RL, et al. Regional white matter volume differences in non-demented aging and Alzheimer's disease. *NeuroImage* 2009; **44**: 1247–58

6 Liu H, Yang Y, Xi Y, Zhu W, Leak RK, Wei Z, et al. Aging of cerebral white matter. *Ageing Res Rev* 2017; **34**: 64–76

7 Marner L, Nyengaard JR, Tang Y, Pakkenberg B. Marked loss of myelinated nerve fibers in the human brain with age. *J Comp Neurol* 2003; **462**: 144–52

8 Gao J, Cheung RT, Lee TM, Chu LW, Chan YS, Mak HK, et al. Possible retrogenesis observed with fiber tracking: an anteroposterior pattern of white matter disintegrity in normal aging and Alzheimer's disease. *J Alzh Dis* 2011; **26**: 47–58

9 Erten-Lyons D, Woltjer R, Kaye J, Mattek N, Dodge HH, Green S, et al. Neuropathologic basis of white matter hyperintensity accumulation with advanced age. *Neurology* 2013; **81**: 977–83

10 Wharton SB, Simpson JE, Brayne C, Ince PG. Age-associated white matter lesions: the MRC Cognitive Function and Ageing Study. *Brain Pathol* 2015; **25**: 35–43

11 Kavroulakis E, Simos PG, Kalaitzakis GA, Maris TG, Karageorgou D, Zaganas I, et al. Myelin content changes in probable Alzheimer's disease and mild cognitive impairment: associations with age and severity of neuropsychiatric impairment. *J Magn Reson Imaging* 2018; **47**: 1359–72

12 Bartzokis G, Cummings JL, Sultzer D, Henderson VW, Nuechterlein KH, Mintz J. White matter structural integrity in healthy aging adults and patients with Alzheimer disease: a magnetic resonance imaging study. *Arch Neurol* 2003; **60**: 393–8

13 Bartzokis G, Sultzer D, Lu PH, Nuechterlein KH, Mintz J, Cummings JL. Heterogeneous age-related breakdown of white matter structural integrity: implications for cortical "disconnection" in aging and

Alzheimer's disease. *Neurobiol Aging* 2004; **25**: 843–51

14 Bennett IJ, Madden DJ. Disconnected aging: cerebral white matter integrity and age-related differences in cognition. *Neuroscience* 2014; **276**: 187–205

15 Sugiyama I, Tanaka K, Akita M, Yoshida K, Kawase T, Asou H. Ultrastructural analysis of the paranodal junction of myelinated fibers in 31-month-old-rats. *J Neurosci Res* 2002; **70**: 309–17

16 Kohama SG, Rosene DL, Sherman LS. Age-related changes in human and non-human primate white matter: from myelination disturbances to cognitive decline. *Age* 2012; **34**: 1093–110

17 Diaz JF, Merskey H, Hachinski VC, Lee DH, Boniferro M, Wong CJ, et al. Improved recognition of leukoaraiosis and cognitive impairment in Alzheimer's disease. *Arch Neurol* 1991; **48**: 1022–25

18 Rose SE, Chen F, Chalk JB, Zelaya FO, Strugnell WE, Benson M, et al. Loss of connectivity in Alzheimer's disease: an evaluation of white matter tract integrity with colour coded MR diffusion tensor imaging. *J Neurol Neurosurg Psychiatry* 2000; **69**: 528–30

19 Wang L, Goldstein FC, Levey AI, Lah JJ, Meltzer CC, Holder CA, et al. White matter hyperintensities and changes in white matter integrity in patients with Alzheimer's disease. *Neuroradiology* 2011; **53**: 373–81

20 Radanovic M, Pereira FR, Stella F, Aprahamian I, Ferreira LK, Forlenza OV, et al. White matter abnormalities associated with Alzheimer's disease and mild cognitive impairment: a critical review of MRI studies. *Expert Rev Neurother* 2013; **13**: 483–93

21 Brickman AM. Contemplating Alzheimer's disease and the contribution of white matter hyperintensities. *Curr Neurol Neurosci Rep* 2013; **13**: 415

22 Joki H, Higashiyama Y, Nakae Y, Kugimoto C, Doi H, Kimura K, et al. White matter hyperintensities on MRI in dementia with Lewy bodies, Parkinson's disease with dementia, and Alzheimer's disease. *J Neurol Sci* 2018; **385**: 99–104

23 Medina D, Urresta F, Gabrieli JD, Moseley M, Fleischman D, Bennett DA, et al. White matter changes in mild cognitive impairment and AD: a diffusion tensor imaging study. *Neurobiol Aging* 2006; **27**: 663–72

24 Selnes P, Fjell AM, Gjerstad L, Bjornerud A, Wallin A, Due-Tonnessen P, et al. White matter imaging changes in subjective and mild cognitive impairment. *Alzheimers Dement* 2012; **8**: S112–21

25 Molinuevo JL, Ripolles P, Simo M, Llado A, Olives J, Balasa M, et al. White matter changes in preclinical Alzheimer's disease: a magnetic resonance imaging diffusion tensor imaging study on cognitively normal older people with positive amyloid beta protein 42 levels. *Neurobiol Aging* 2014; **35**: 2671–2680

26 Hoy AR, Ly M, Carlsson CM, Okonkwo OC, Zetterberg H, Blennow K, et al. Microstructural white matter alterations in preclinical Alzheimer's disease detected using free water elimination diffusion tensor imaging. *PLoS One* 2017; **12**: e0173982

27 Bouhrara M, Reiter DA, Bergeron CM, Zukley LM, Ferrucci L, Resnick SM, Spencer RG. Evidence of demyelination in mild cognitive impairment and dementia using a direct and specific magnetic resonance imaging measure of myelin content. *Alzheimers Dement* 2018; **14**: 998–1004

28 Lee S, Viqar F, Zimmerman ME, Narkhede A, Tosto G, Benzinger TL, et al. White matter hyperintensities are a core feature of Alzheimer's disease: evidence from the dominantly inherited Alzheimer network. *Ann Neurol* 2016; **79**: 929–39

29 de la Monte SM. Quantitation of cerebral atrophy in preclinical and end-stage Alzheimer's disease. *Ann Neurol* 1989; **25**: 450–59

30 Sjobeck M, Haglund M, Englund E. Decreasing myelin density reflected increasing white matter pathology in Alzheimer's disease – a neuropathological study. *Int J Geriatr Psychiatry* 2005; **20**: 919–26

31 Gouw AA, Seewann A, Vrenken H, van der Flier WM, Rozemuller JM, Barkhof F, et al. Heterogeneity of white matter hyperintensities in Alzheimer's disease: post-mortem quantitative MRI and neuropathology. *Brain* 2008; **131**: 3286–98

32 Ihara M, Polvikoski TM, Hall R, Slade JY, Perry RH, Oakley AE, et al. Quantification of myelin loss in frontal lobe white matter in vascular dementia, Alzheimer's disease, and dementia with Lewy bodies. *Acta Neuropathol* 2010; **119**: 579–89

33 Reisberg B, Franssen EH, Souren LE, Auer SR, Akram I, Kenowsky S. Evidence and mechanisms of retrogenesis in Alzheimer's and other dementias: management and treatment import. *Am J Alzheimers Dis Other Demen* 2002; **17**: 202–12

34 Benitez A, Fieremans E, Jensen JH, Falangola MF, Tabesh A, Ferris SH, et al. White matter tract integrity metrics reflect the vulnerability of late-myelinating tracts in Alzheimer's disease. *Neuroimage Clin* 2014; **4**: 64–71

35 Jellinger KA. The enigma of vascular cognitive disorder and vascular dementia. *Acta Neuropathol* 2007; **113**: 349–88

36 Ferrer I. Cognitive impairment of vascular origin: neuropathology of cognitive impairment. *J Neurol Sci* 2010; **299**: 139–49

37 Thal DR, Grinberg TL, Attems J. Vascular dementia: different forms of vessel disorders contribute to the development of dementia in the elderly brain. *Exp Gerontol* 2012; **47**: 816–24

38 Kalaria RN. Neuropathological diagnosis of vascular cognitive impairment and vascular dementia with implications for Alzheimer's disease. *Acta Neuropathol* 2016; **131**: 659–85

39 McAleese KE, Alafuzoff I, Charidimou A, De Reuck J, Grinberg LT, Hainsworth AH, et al. Post-mortem

assessment in vascular dementia: advances and aspirations. *BMC Med* 2016; **14**: 129

40 Skrobot OA, Attems J, Esiri M, Hortobágyi T, Ironside JW, Kalaria RN, et al. Vascular cognitive impairment neuropathology guidelines (VCING): the contribution of cerebrovascular pathology to cognitive impairment. *Brain* 2016; **139**: 2957–69

41 Khan A, Kalaria RN, Corbett A, Ballard C. Update on vascular dementia. *J Geriatr Psychiatry Neurol* 2016; **29**: 281–301

42 Vinters HV, Zarow C, Borys E, Whitman JD, Tung S, Ellis WG, et al. Review: vascular dementia: clinico-pathologic and genetic considerations. *Neuropathol Appl Neurobiol* 2018; **44**: 247–66

43 Delay J, Brion S. *Les Demences Tardives*. Paris: Masson & Cie, 1962

44 Tomlinson BE, Blessed G, Roth M. Observations on the brains of demented people. *J Neurol Sci* 1970; **11**: 205–42

45 Snowdon DA, Greiner LH, Mortimer JA, Riley KP, Greiner PA, Markesbery WR. Brain infarction and the clinical expression of Alzheimer's disease. The Nun Study. *JAMA* 1997; **277**: 813–17

46 Schneider JA, Wilson RS, Bienias JL, Evans DA, Bennett DA. Cerebral infarction and the likelihood of dementia from Alzheimer disease pathology. *Neurology* 2004; **62**: 1148–55

47 Chui HC, Zarow C, Mack WJ, Elis WG, Zheng L, Jagust WJ, et al. Vinters HV. Cognitive impact of subcortical vascular and Alzheimer's disease pathology. *Ann Neurol* 2006; **60**: 677–87

48 Jellinger KA. The enigma of mixed dementia. *Alzheimers Dement* 2007; **3**: 40–53

49 Ferrer I, Vidal N. Neuropathology of cerebrovascular diseases. *Handb Clin Neurol* 2017; **145**: 79–114

50 Magaki S, Yong WH, Khanlou N, Tung S, Vinters HV. Comorbidity in dementia: update of an ongoing autopsy study. *J Am Geriatr Soc* 2014; **62**: 1722–8

51 White LR, Edland SD, Hemmy LS, Montine KS, Zarow C, Sonnen JA, et al. Neuropathologic comorbidity and cognitive impairment in the Nun and Honolulu-Asia Aging Studies. *Neurology* 2016; **86**: 1000–8

52 Haaksma ML, Vilela LR, Marengoni A, Calderón-Larrañaga A, Leoutsakos JS, Olde Rikkert MGM, et al. Comorbidity and progression of late onset Alzheimer's disease: a systematic review. *PLoS One* 2017; **12**: e0177044

53 Alafuzoff I, Kovacs GG. Comorbidities. *Handb Clin Neurol* 2017; **145**: 573–7

54 Karki R, Kodamullil AT, Hofmann-Apitius M. Comorbidity analysis between Alzheimer's disease and type 2 diabetes mellitus based on shared pathways and the role of T2DM drugs. *J Alzheimers Dis* 2017; **60**: 721–31

55 Wang JH, Wu YJ, Tee BL, Lo RY. Medical comorbidity in Alzheimer's disease: a nested case-control study. *J Alzheimers Dis* 2018; **63**: 773–81

56 Mendes A, Tezenas du Montcel S, Levy M, Bertrand A, Habert MO, Bertin H, et al. Multimorbidity is associated with preclinical Alzheimer's disease neuroimaging biomarkers. *Dement Geriatr Cogn Disord* 2018; **45**: 272–81

57 Tripathi RB, Rivers LE, Young KM, Jamen F, Richardson WD. NG2 glia generate new oligodendrocytes but few astrocytes in a murine experimental autoimmune encephalomyelitis model of demyelinating disease. *J Neurosci* 2010; **30**: 16383–90

58 Zawadzka M, Rivers LE, Fancy SP, Zhao C, Tripathi R, Jamen F, et al. CNS-resident glial progenitor/stem cells produce Schwann cells as well as oligodendrocytes during repair of CNS demyelination. *Cell Stem Cell* 2010; **6**: 578–90

59 Tognata R, Miller RH. Contribution of the oligodendrocyte lineage to CNS repair and neurodegenerative pathologies. *Neuropharmacology* 2016; **110**: 539–47

60 Liu Z, Hu X, Cai J, Liu B, Peng X, Wegner M, et al. Induction of oligodendrocyte differentiation by Olig2 and Sox10: evidence for reciprocal interactions and dosage-dependent mechanisms. *Developl biol* 2007; **302**: 683–93

61 Cahoy JD, Emery B, Kaushal A, Foo LC, Zamanian JL, Christopherson KS, et al. A transcriptome database for astrocytes, neurons, and oligodendrocytes: a new resource for understanding brain development and function. *J Neurosci* 2008; **28**: 264–78

62 Emery B, Agalliu D, Cahoy JD, Watkins TA, Dugas JC, Mulinyawe SB, et al. Myelin gene regulatory factor is a critical transcriptional regulator required for CNS myelination. *Cell* 2009; **138**: 172–185

63 Jahn O, Tenzer S, Werner HB. Myelin proteomics: molecular anatomy of an insulating sheath. *Mol Neurobiol* 2009; **40**: 55–72

64 Llorens F, Gil V, del Río JA. Emerging functions of myelin-associated proteins during development, neuronal plasticity, and neurodegeneration. *FASEB J* 2011; **25**: 463–75

65 Koenning M, Jackson S, Hay CM, Faux C, Kilpatrick TJ, Willingham M, Emery B. Myelin gene regulatory factor is required for maintenance of myelin and mature oligodendrocyte identity in the adult CNS. *J Neurosci* 2012; **32**: 12528–42

66 Bujalka H, Koenning M, Jackson S, Perreau VM, Pope B, Hay CM, et al. MYRF is a membrane-associated transcription factor that autoproteolytically cleaves to directly activate myelin genes. *PLoS Biol* 2013; **11**: e1001625

67 Raasakka A, Kursula P. The myelin membrane-associated enzyme 2',3'-cyclic nucleotide 3'-phosphodiesterase: on a highway to structure and function. *Neurosci Bull* 2014; **30**: 956–66

68 McKerracher L, Rosen KM. MAG, myelin and overcoming growth inhibition in the CNS. *Front Mol Neurosci* 2015; **8**: 51

69 Pierre K, Pellerin L. Monocarboxylate transporters in the central nervous system: distribution, regulation and function. *J Neurochem* 2005; **94**: 1–14

70 Saab AS, Tzvetanova ID, Nave K-A. The role of myelin and oligodendrocytes in axonal energy metabolism. *Curr Opin Neurobiol* 2013; **23**: 1065–72

71 Rinholm JE, Hamilton NB, Kessaris N, Richardson WD, Bergersen LH, Attwell D. Regulation of oligodendrocyte development and myelination by glucose and lactate. *J Neurosci* 2011; **31**: 538–48

72 Lee Y, Morrison BM, Li Y, Lengacher S, Farah MH, Hoffman PN, et al. Oligodendroglia metabolically support axons and contribute to neurodegeneration. *Nature* 2012; **487**: 443–48

73 Ye F, Chen Y, Hoang T, Montgomery RL, Zhao XH, Bu H, et al. HDAC1 and HDAC2 regulate oligodendrocyte differentiation by disrupting the beta-catenin-TCF interaction. *Nat Neurosci* 2009; **12**: 829–38

74 Yao ZG, Zhang L, Huang L, Zhu H, Liu Y, Ma CM, et al. Regional and cell-type specific distribution of HDAC2 in the adult mouse brain. *Brain Struct Funct* 2013; **218**: 563–73

75 Ferrer I. Brain banking. In *Encyclopedia of the Neurological Sciences* 2nd edn, vol. **1**. Eds MJ Aminoff, RB Daroff. Oxford: Academic Press, 2014; 467–73

76 Braak H, Braak E. Neuropathological stageing of Alzheimer-related changes. *Acta Neuropathol* 1991; **82**: 239–59

77 Barrachina M, Castaño E, Ferrer I. TaqMan PCR assay in the control of RNA normalization in human post-mortem brain tissue. *Neurochem Int* 2006; **49**: 276–84

78 Ferrer I. Diversity of astroglial responses across human neurodegenerative disorders and brain aging. *Brain Pathol* 2017; **27**: 645–74

79 Braak H, Thal DR, Ghebremedhin E, Del Tredici K. Stages of the pathologic process in Alzheimer disease: age categories from 1 to 100 years. *J Neuropathol Exp Neurol* 2011; **70**: 960–69

80 Ferrer I. Defining Alzheimer as a common age-related neurodegenerative process not inevitably leading to dementia. *Prog Neurogibol* 2012; **97**: 38–51

81 Crary JF, Trojanowski JQ, Schneider JA, Abisambra JF, Abner EL, Alafuzoff I, , et al. Primary age-related tauopathy (PART): a common pathology associated with human aging. *Acta Neuropathol* 2014; **128**: 755–66

82 Duyckaerts C, Braak H, Brion JP, et al. PART is part of Alzheimer disease. *Acta Neuropathol* 2015; **129**: 49–756

83 Yokoi S, Nakano T, Suzuki K. Studies in the white matter of Alzheimer's disease-morphological, lipid-chemical investigation. *No To Shinkei* 1982; **34**: 1197–205

84 Soderberg M, Edlund C, Alafuzoff I, Kristensson K, Dallner G. Lipid composition in different regions of the brain in Alzheimer's disease/senile dementia of Alzheimer's type. *J Neurochem* 1992; **59**: 1646–53

85 Svennerholm L, Gottfries CG. Membrane lipids, selectively diminished in Alzheimer brains, suggest synapse loss as a primary event in early-onset form (type I) and demyelination in late-onset form (type II). *J Neurochem* 1994; **62**: 1039e1047

86 Roher AE, Weiss N, Kokjohn TA, Kuo YM, Kalback W, Anthony J, et al. Increased Aβ peptides and reduced cholesterol and myelin proteins characterize white matter degeneration in Alzheimer's disease. *Biochemistry* 2002; **41**: 11080–90

87 Han X, Holtzman DM, McKeel DW, Kelley J, Morris JC. Substantial sulfatide deficiency and ceramide elevation in very early Alzheimer's disease: potential role in disease pathogenesis. *J Neurochem* 2002; **82**: 809e818

88 Hejazi L, Wong JW, Cheng D, Proschogo N, Ebrahimi D, Garner B, et al. Mass and relative elution time profiling: two-dimensional analysis of sphingolipids in Alzheimer's disease brains. *Biochem J* 2011; **438**: 165e175

89 Couttas TA, Kain N, Suchowerska AK, Turner N, Fath T, Garner B, et al. Loss of ceramide synthase 2 activity, necessary for myelin biosynthesis, precedes tau pathology in the cortical pathogenesis of Alzheimer's disease. *Neurobiol Aging* 2016; **43**: 89e100

90 Vlkolinsky R, Cairns N, Fountoulakis M, Lubec G. Decreased brain levels of 2′,3′-cyclic nucleotide-3′-phosphodiesterase in Down syndrome and Alzheimer's disease. *Neurobiol Aging* 2001; **22**: 547–53

91 Caso F, Agosta F, Filippi M. Insights into white matter damage in Alzheimer's disease: from post-mortem to in vivo diffusion tensor MRI studies. *Neurodegener Dis* 2016; **16**: 26–33

92 Xu J, Chen S, Ahmed SH, Chen H, Ku G, Goldberg MP, et al. Amyloid-beta peptides are cytotoxic to oligodendrocytes. *J Neurosci* 2001; **21**: Rc118

93 Lee JT, Xu J, Lee JM, Ku G, Han X, Yang DI, et al. Amyloid beta peptide induces oligodendrocyte death by activating the neutral sphingomyelinase-ceramide pathway. *J Cell Biol* 2004; **164**: 123–31

94 Jantaratnotai N, Ryu JK, Kim SU, McLarnon JG. Amyloid beta peptide induced corpus callosum damage and glial activation in vivo. *NeuroReport* 2003; **14**: 1429–33

95 Billings LM, Oddo S, Green KN, McGaugh JL, LaFerla FM. Intraneuronal Aβ causes the onset of early Alzheimer's disease-related cognitive deficits in transgenic mice. *Neuron* 2005; **45**: 675–88

96 Chu TH, Cummins K, Sparling JS, Tsutsui S, Brideau C, Nilsson KPR, et al. Axonal and myelinic pathology in 5xFAD Alzheimer's mouse spinal cord. *PLoS One* 2017; **12**: e0188218

97 Quintela-López T, Ortiz-Sanz C, Serrano-Regal MP, Gaminde-Blasco A, Valero J, Baleriola J, et al. Aβ

oligomers promote oligodendrocyte differentiation and maturation via integrin β1 and Fyn kinase signaling. *Cell Death Dis* 2019; **10**: 445

98 Roseborough A, Ramirez J, Black SE, Edwards JD. Associations between amyloid β and white matter hyperintensities: a systematic review. *Alzheimers Dement* 2017; **13**: 1154–67

99 Collins-Praino LE, Francis YI, Griffith EY, Wiegman AF, Urbach J, Lawton A, et al. Soluble amyloid beta levels are elevated in the white matter of Alzheimer's patients, independent of cortical plaque severity. *Acta Neuropathol Commun* 2014; **2**: 83

100 McAleese KE, Firbank M, Dey M, Colloby SJ, Walker L, Johnson M, et al. Cortical tau load is associated with white matter hyperintensities. *Acta Neuropathol Commun* 2015; **3**: 60

101 McAleese KE, Walker L, Graham S, Moya ELJ, Johnson M, Erskine D, et al. Parietal white matter lesions in Alzheimer's disease are associated with cortical neurodegenerative pathology, but not with small vessel disease. *Acta Neuropathol* 2017; **134**: 459–73

102 Stokin GB, Lillo C, Falzone TL, Brusch RG, Rockenstein E, Mount SL, et al. Axonopathy and transport deficits early in the pathogenesis of Alzheimer's disease. *Science* 2005; **307**: 1282–88

103 Sahara N, Perez PD, Lin WL, Dickson DW, Ren Y, Zeng H, et al. Age-related decline in white matter integrity in a mouse model of tauopathy: an *in vivo* diffusion tensor magnetic resonance imaging study. *Neurobiol Aging* 2014; **35**: 1364e1374

104 Gagyi E, Kormos B, Castellanos KJ, Valyi-Nagy K, Korneff D, LoPresti P, et al. Decreased oligodendrocyte nuclear diameter in Alzheimer's disease and Lewy body dementia. *Brain Pathol* 2012; **22**: 803–10

105 Behrendt G, Baer K, Buffo A, Curtis MA, Faull RL, Rees MI, et al. Dynamic changes in myelin aberrations and oligodendrocyte generation in chronic amyloidosis in mice and men. *Glia* 2013; **61**: 273–86

106 Nielsen HM, Ek D, Avdic U, Orbjorn C, Hansson O, Netherlands Brain B; Veerhuis R, et al. NG2 cells, a new trail for Alzheimer's disease mechanisms? *Acta Neuropathol Commun* 2013; **1**: 7

107 Al-Mashhadi S, Simpson JE, Heath PR, Dickman M, Forster G, Matthews FE, et al. Oxidative glial cell damage associated with white matter lesions in the aging human brain. *Brain Pathol* 2015; **25**: 565–74

108 Tse KH, Herrup K. DNA damage in the oligodendrocyte lineage and its role in brain aging. *Mech Ageing Dev* 2017; **161**: 37–50

109 Rivera A, Vanzuli I, Arellano JJ, Butt A. Decreased regenerative capacity of oligodendrocyte progenitor cells (NG2-Glia) in the ageing brain: a vicious cycle of synaptic dysfunction, myelin loss and neuronal disruption? *Curr Alzheimer Res* 2016; **13**: 413–18

110 Butt AM, Chacon de la Rocha I, Rivera A. Oligodendroglial cells in Alzheimer's disease. In *Neuroglia in Neurodegenerative Diseases*. Eds A Verkhratsky, MS Ho, R Zorec, V Parpura. Singapore: Springer Nature, 2019, 325–34.

111 Pak K, Chan SL, Mattson MP. Presenilin-1 mutation sensitizes oligodendrocytes to glutamate and amyloid toxicities, and exacerbates white matter damage and memory impairment in mice. *NeuroMolecular Med* 2003; **3**: 53–64

112 Desai MK, Sudol KL, Janelsins MC, Mastrangelo MA, Frazer ME, Bowers WJ. Triple-transgenic Alzheimer's disease mice exhibit region-specific abnormalities in brain myelination patterns prior to appearance of amyloid and tau pathology. *Glia* 2009; **57**: 54–65

113 Desai MK, Mastrangelo MA, Ryan DA, Sudol KL, Narrow WC, Bowers WJ. Early oligodendrocyte/myelin pathology in Alzheimer's disease mice constitutes a novel therapeutic target. *Am J Pathol* 2010; **177**: 1422–35

114 Dong XX, Zhang HY, Li HY, Liu PH, Sui Y, Sun XH. Association between Alzheimer's disease pathogenesis and early demyelination and oligodendrocyte dysfunction. *Neural Regen Res* 2018; **13**: 908–14

115 Gu L, Wu D, Tang X, Qi X, Li X, Bai F, et al. Myelin changes at early stage of 5xFAD nice. *Brain Res Bull* 2018; **137**: 285–293

116 Kamphuis W, Orre M, Kooijman L, Dahmen M, Hol EM. Differential cell proliferation in the cortex of the APPswePS1dE9 Alzheimer's disease mouse model. *Glia* 2012; **60**: 615–29

117 Ferrer I, Bella R, Serrano MT, Martí E, Guionnet N. Arteriolosclerotic leucoencephalopathy in the elderly and its relation to white matter lesions in Binswanger's disease, multi-infarct encephalopathy and Alzheimer's disease. *J Neurol Sci* 1990; **98**: 37–50

118 Moody DM, Bell MA, Challa VR. Features of the cerebral vascular pattern that predict vulnerability to perfusion or oxygenation deficiency: an anatomic study. *Am J Neuroradiol* 1990; **11**: 431–39

119 Brown WR, Moody DM, Challa VR, Thore CR, Anstrom JA. Venous collagenosis and arteriolar tortuosity in leukoaraiosis. *J Neurol Sci* 2002; **203–204**: 159–63

120 Grinberg LT, Thal DR. Vascular pathology in the aged human brain. *Acta Neuropathol* 2010; **119**: 277–290

121 Brown WR, Thore CR. Review: cerebral microvascular pathology in ageing and neurodegeneration. *Neuropathol Appl Neurobiol* 2011; **37**: 56–74

122 Bridges LR, Andoh J, Lawrence AJ, Khoong CHL, Poon W, Esiri MM, et al. Blood-brain dysfunction and cerebral small vessel disease (arteriolosclerosis) in brains of older people. *J Neuropathol Exp Neurol* 2014; **73**: 1026–33

123 Liua H, Yanga Y, Xiaa Y, Zhua W, Leakd RK, Weia Z, et al. Aging of cerebral white matter. *Ageing Res Rev* 2017; **34**: 64–76

124 Kalaria RN, Premkumar DR, Pax AB, Cohen DL, Lieberburg I. Production and increased detection of amyloid beta protein and amyloidogenic fragments in brain microvessels, meningeal vessels and choroids plexus in Alzheimer's disease. *Mol Brain Res* 1996; **35**: 58–68

125 Thal DR, Griffin WS, de Vos RA, Ghebremedhin E. Cerebral amyloid angiopathy and its relationship to Alzheimer's disease. *Acta Neuropathol* 2008; **115**: 599–609

126 Silverberg GD, Messier AA, Miller MC, Machan JT, Majmudar SS, Stopa EG, , et al. Amyloid efflux transporter expression at the blood-brain barrier declines in normal aging. *J Neuropathol Exp Neurol* 2010; **69**: 1034–1043

127 Silverberg GD, Miller MC, Messier AA, Majmudar S, Machan JT, Donahue JE, et al. Amyloid deposition and influx transporter expression at the blood-brain barrier increase in normal aging. *J Neuropathol Exp Neurol* 2010; **69**: 98–108

128 Kalaria RN, Pax AB. Increased collagen content of cerebral microvessels in Alzheimer's disease. *Brain Res* 1995; **707**: 349–52

129 Farkas E, Luiten PGM. Cerebral microvascular pathology in aging and Alzheimer's disease. *Progr Neurobiol* 2001; **64**: 575–611

130 Grammas P, Yamada M, Zlokovic B. The cerebromicrovasculature: a key player in the pathogenesis of Alzheimer's disease. *J Alzheimers Dis* 2002; **4**: 217–23

131 Ervin JF, Pannell C, Szymansky M, Welsh-Bohmer K, Schmechel DE, Hulette CM. Vascular smooth muscle actin is reduced in Alzheimer disease brain: a quantitative analysis. *J Neuropathol Exp Neurol* 2004; **63**: 735–41

132 Perez E, Barrachina M, Rodriguez A, Torrejón-Escribano B, Boada M, Hernandez I, et al. Aquaporin expression in the cerebral cortex is increased at early stages of Alzheimer's disease. *Brain Res* 2007; **1128**: 164–74

133 Anderson VC, Lenar DP, Quinn JF, Rooney WD. The blood-brain barrier and microvascular water exchange in Alzheimer's disease. *Cardiovasc Psychiatry Neurol* 2011; **2011**: 615829

134 Erickson MA, Banks WA. Blood–brain barrier dysfunction as a cause and consequence of Alzheimer's disease. *J Cereb Blood Flow Metab* 2013; **33**: 1500–13

135 Zenaro E, Piacentino G, Constantin G. The blood-brain barrier in Alzheimer's disease. *Neurobiol Dis* 2017; **107**: 41–56

136 Gallart-Palau X, Serra A, Hase Y, Tan CF, Chen CP, Kalaria RN, et al. Brain-derived and circulating vesicle profiles indicate neurovascular unit dysfunction in early Alzheimer's disease. *Brain Pathol* 2019; **29**: 593–605

137 Scheibel AB, Duong TH, Jacobs R. Alzheimer's disease as a capillary dementia. *Ann Med* 1989; **21**: 103–7

138 De la Torre JC. Alzheimer's disease is a vasocognopathy: a new term to describe its nature. *Neurol Res* 2004; **26**: 517–24

139 Kalback W, Esh C, Castano EM, Rahman A, Kojohn T, Luehrs DC, et al. Atherosclerosis, vascular amyloidosis and brain hypoperfusion in the pathogenesis of sporadic Alzheimer's disease. *Neurol Res* 2004; **26**: 525–9

140 Bartzokis G. Alzheimer's disease as homeostatic responses to age-related myelin breakdown. *Neurobiol Aging* 2011; **32**: 1341–71

141 Cai Z, Xiao M. Oligodendrocytes and Alzheimer's disease. *Int J Neurosci* 2016; **126**: 97–104

142 Nasrabady SE, Rizvi B, Goldman JE, Brickman AM. White matter changes in Alzheimer's disease: a focus on myelin and oligodendrocytes. *Acta Neuropathol Commun* 2018; **6**: 22

143 Mot AI, Depp C, Nave KA. An emerging role of dysfunctional axon-oligodendrocyte coupling in neurodegenerative diseases. *Dialogues Clin Neurosci* 2018; **20**: 283–92

144 Ferrer I. Oligodendrogliopathy in neurodegenerative diseases with abnormal protein aggregates: the forgotten partner. *Prog Neurogibol* 2018; **169**: 24–54